**SUPPLEMENTARY INFORMATION**

# Identification of copper-containing oxidoreductases in the secretomes of three *Colletotrichum* species with a focus on copper radical oxidases for the biocatalytic production of fatty aldehydes

*David Ribeaucourt[1,2,3], Safwan Saker[1,a], David Navarro[1], Bastien Bissaro[1], Elodie Drula[1,4,5], Lydie Oliveira Correia[6], Mireille Haon[1], Sacha Grisel[1], Nicolas Lapalu[7], Bernard Henrissat[4,5,8], Richard J. O'Connell[7], Fanny Lambert[3], Mickaël Lafond[2*] and Jean-Guy Berrin[1*]*

[1]INRAE, Aix Marseille Univ, UMR1163 Biodiversité et Biotechnologie Fongiques, Marseille, France

[2]Aix Marseille Univ, CNRS, Centrale Marseille, iSm2, Marseille, France

[3]V. Mane Fils, 620 route de Grasse, Le Bar sur Loup, France

[4]INRAE, USC1408, AFMB, Marseille, France

[5]CNRS, Aix Marseille Univ, UMR7257, AFMB, Marseille, France

[6]Plateforme d'Analyse Protéomique de Paris Sud-Ouest, INRAE, AgroParisTech, Université Paris-Saclay, Micalis Institute, Jouy-en-Josas, France

[7]UMR BIOGER, Institut National de la Recherche Agronomique, AgroParisTech, Université Paris-11Saclay, Versailles, France

[8]Department of Biological Sciences, King Abdulaziz University, Jeddah, Saudi Arabia

[a]present address: CRITT BOIS, Epinal, France

*corresponding authors:

Jean-Guy Berrin (jean-guy.berrin@inrae.fr)
Mickaël Lafond (mickael.lafond@univ-amu.fr)

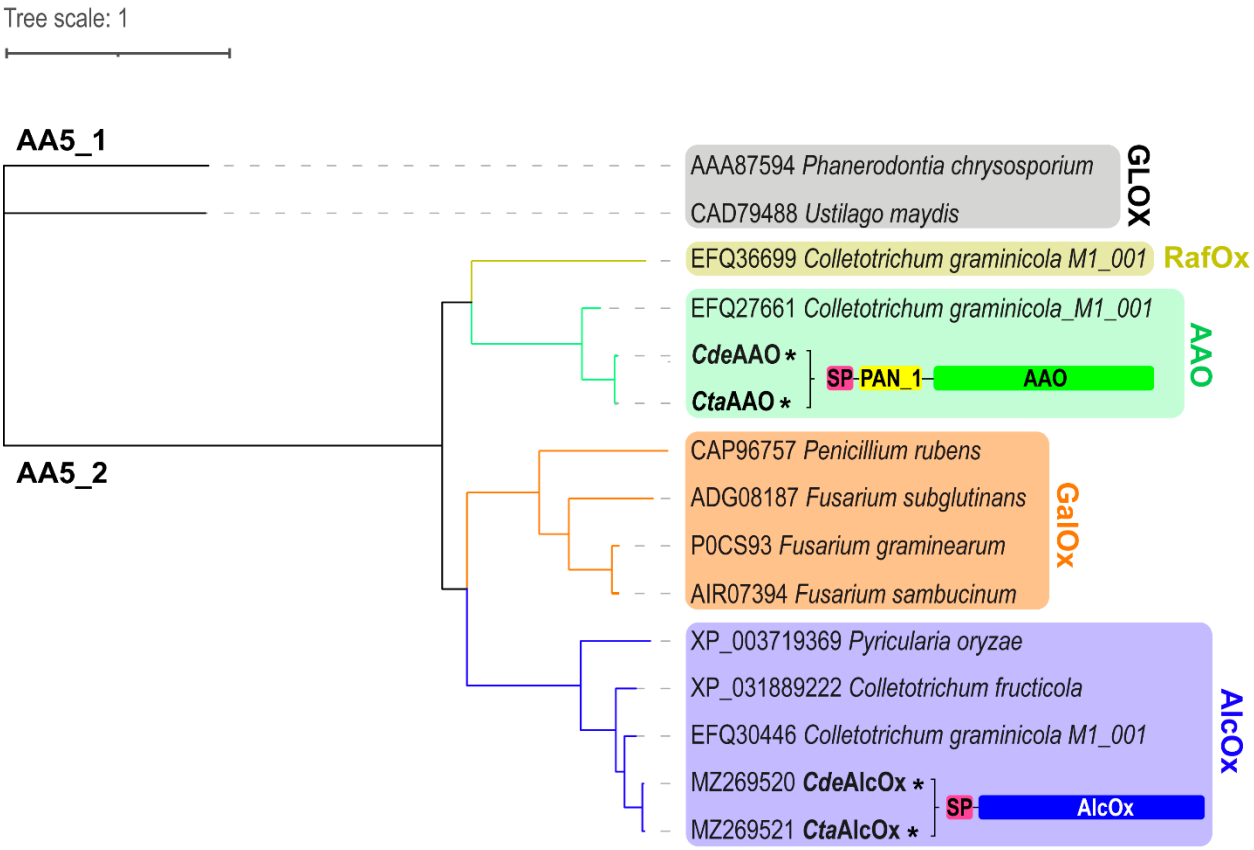


**Figure S1: Phylogenetic tree representation for the alignment of *C. destructivum* and *C. tabacum* AA5_2 (displayed in bold characters and marked with an asterisk) with some of the characterized AA5_2s.** The tree was derived from a multiple sequence alignment. The modularity of the *Cde*- and *Cta*AA5_2 is represented next to their name; Abbreviations: SP,signal peptide; GLOX, Glyoxal oxidase; RafOx, Raffinose oxidase (1).

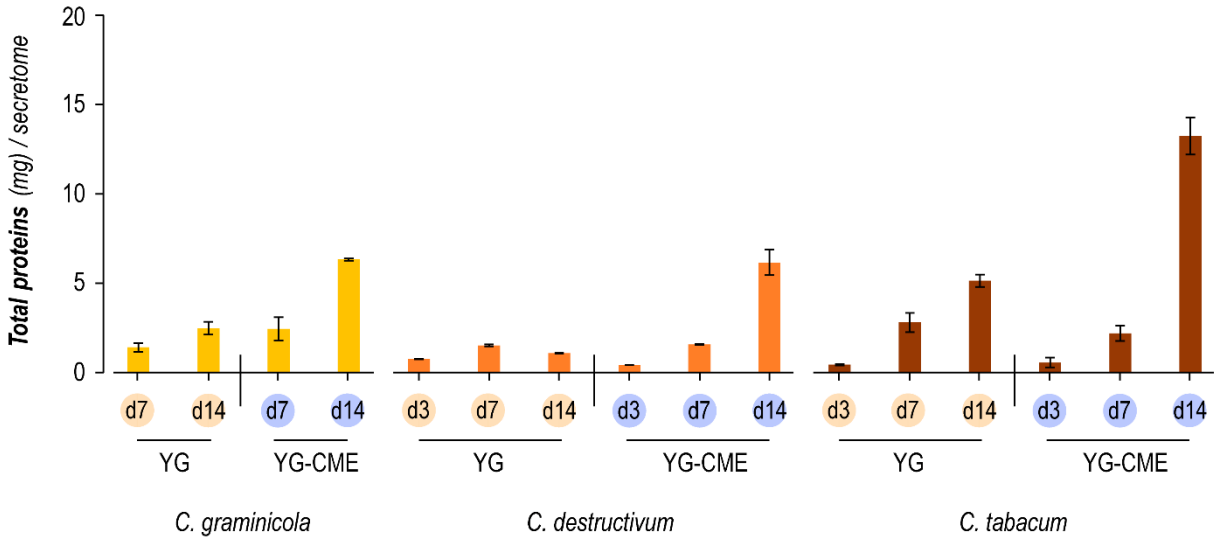


**Figure S2. Quantification of total soluble proteins in *Colletotrichum* secretomes using the Bradford assay and BSA as standard.** The total volume of each secretome was 300 mL. Error bars show independent experiment (n=2).

**A**

| CAZyme (% of total PAI) | YG | | | YG-CME | | |
|---|---|---|---|---|---|---|
| | d3 | d7 | d14 | d3 | d7 | d14 |
| *C. graminicola* | - | 46.4 | 43.3 | - | 43.1 | 47.5 |
| *C. destructivum* | 36.2 | 29.3 | 32.4 | 36.2 | 30.4 | 29.1 |
| *C. tabacum* | 41.4 | 50.3 | 48.6 | 50.9 | 52.1 | 50.5 |

**B**

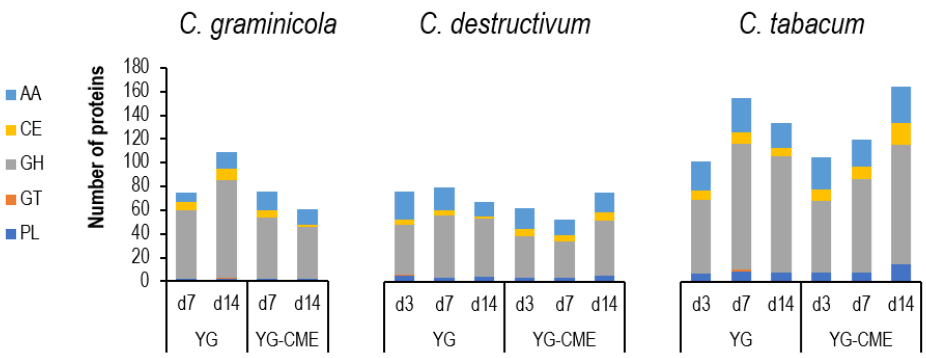


**Figure S3. CAZymes identified in the *Colletotrichum* secretomes. (A)** relative abundance of CAZymes in the secretomes (expressed in percentage of total PAI). **(B)** Number of unique CAZymes identified in the secretomes. Abbreviations: PAI, Protein Abundance Index; AA, auxiliary activities; CE, carbohydrate esterases ; GH, glycoside hydrolases; GT, glycosyl transferases; PL, polysaccharide lyases.

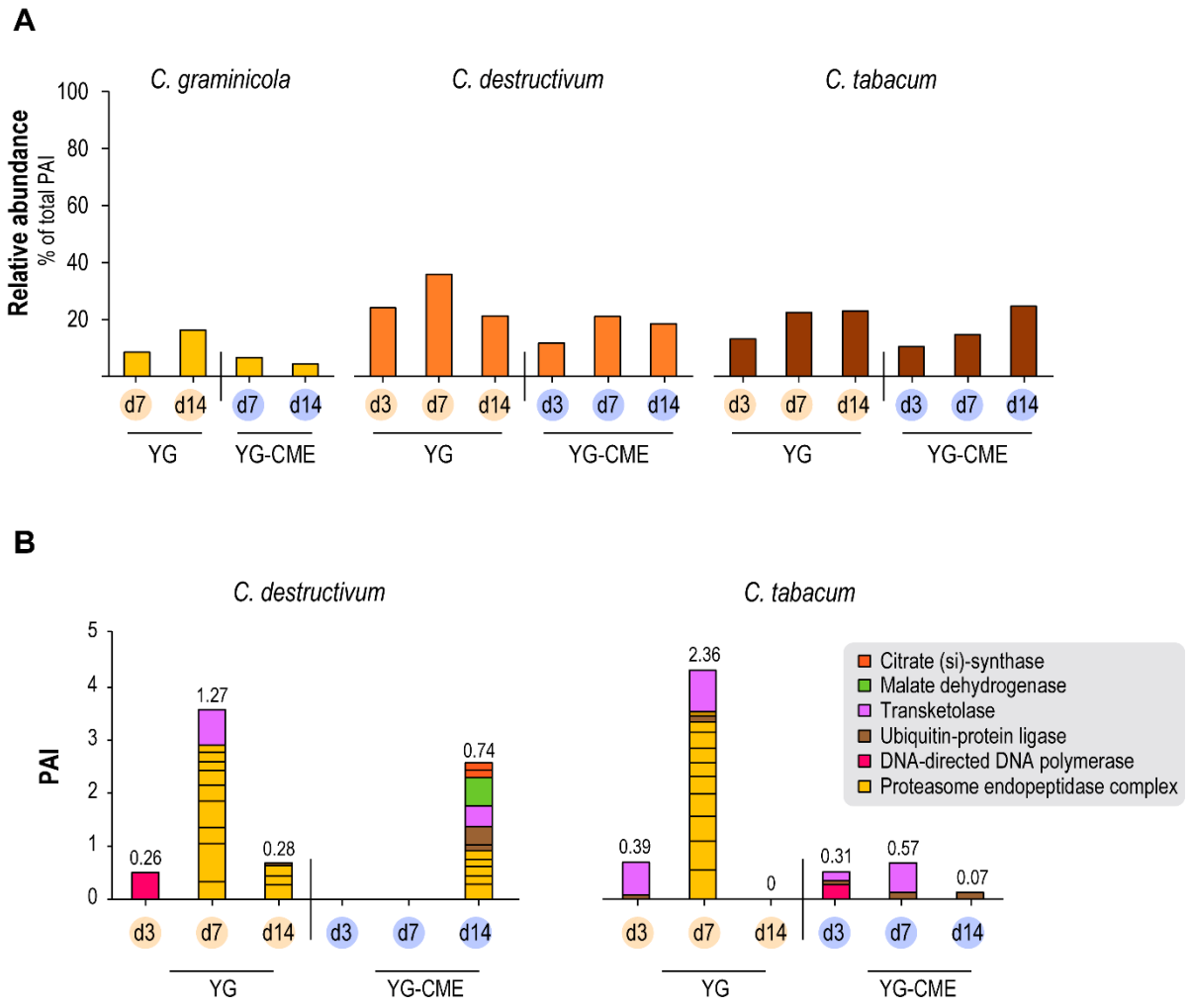


**Figure S4. Abundancy of intracellular proteins in *Colletotrichum* secretomes. (A)** Proportion of proteins predicted without signal peptide (expressed in percentage of total PAI) and detected in the secretomes. **(B)** abundancy of various intracellular proteins used as marker of cell lysis. The number displayed at the top of each bar in panel B corresponds to the relative percentage of the selected proteins against total PAI of each secretome. Note: none of the selected proteins were found in *C. graminicola* secretomes.

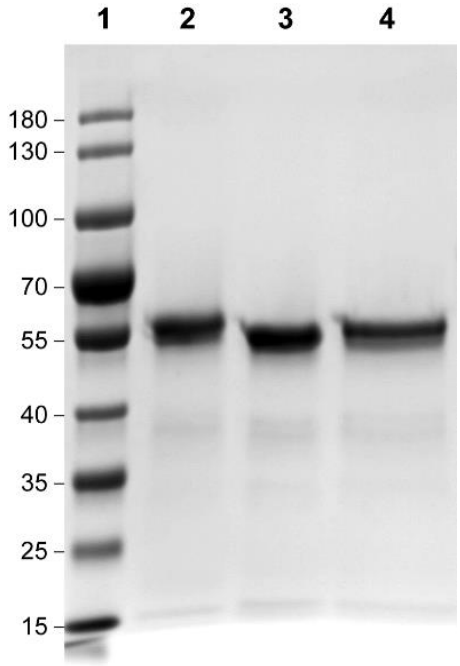


**Figure S5**. **SDS-PAGE of purified recombinant AA5_2 AlcOx.** Lanes 1: molecular weight marker (PageRuler – Thermo Scientific; size expressed in kDa), 2: *Cgr*AlcOx, 3: *Cta*AlcOx, 4: *Cde*AlcOx. 3 µg of each enzyme were loaded on a 10 % polyacrylamide gel. Gel was stained by Coomassie blue and displayed as grey shades.

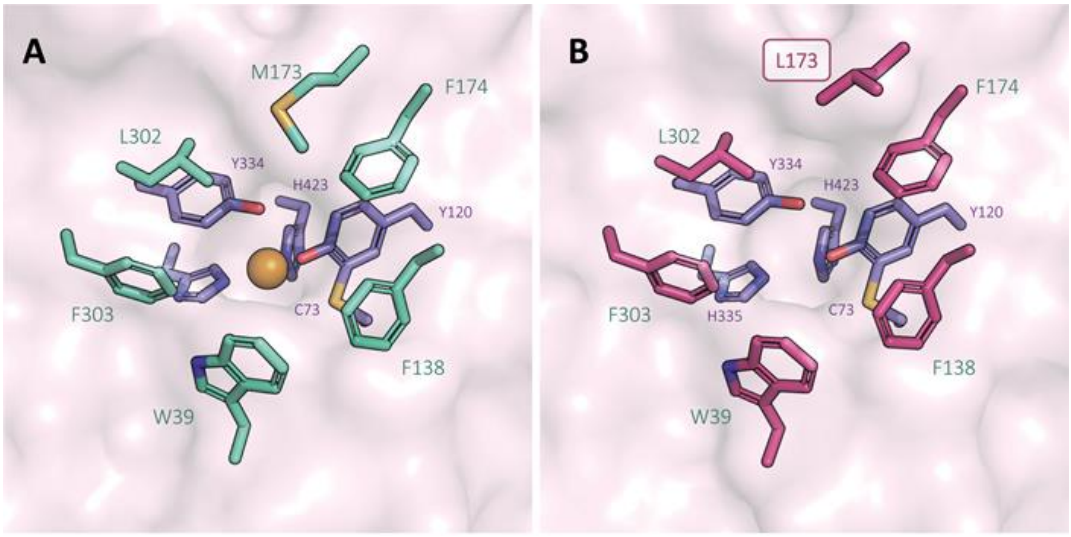


**Figure S6. Structural view of the copper-binding centers of (A) *Cgr*AlcOx (PDB ID 5C92** (2)**), and (B) *Cde*AlcOx (homology model).** The active site amino acid natural substitution in *Cde*AlcOx (compared to *Cgr*AlcOx) is framed and highlighted. The *Cde*AlcOx model was generated through Phyre2 web portal (3).

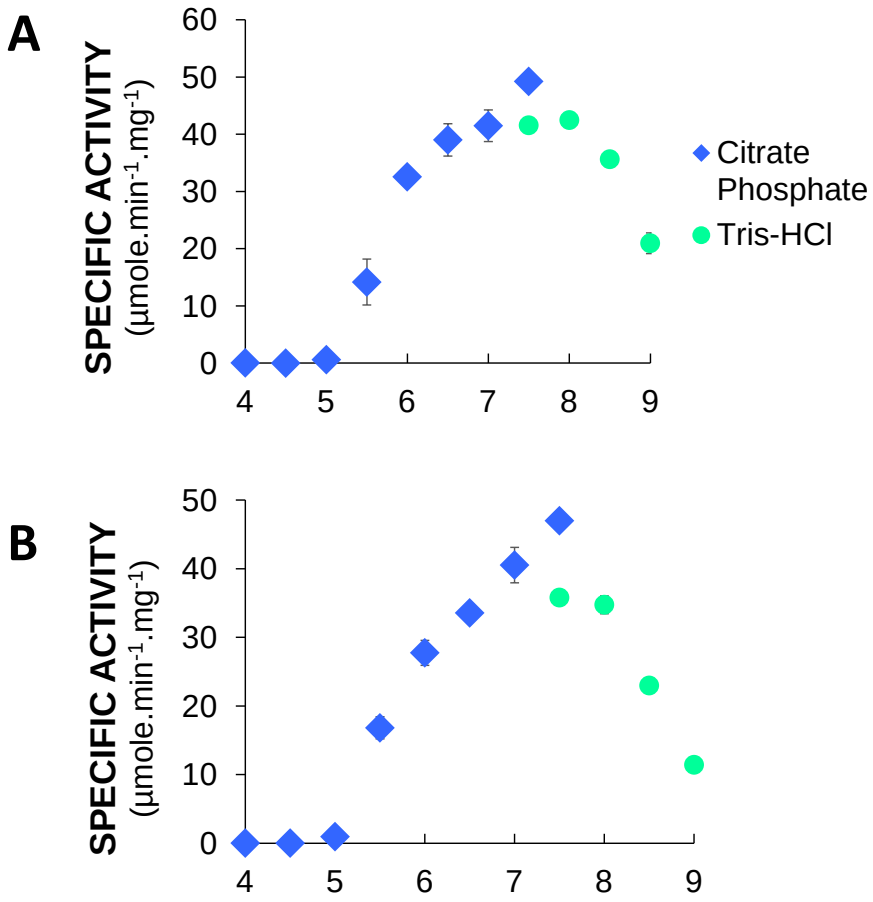


**Figure S7: pH-rate profiles of (A) *Cta*AlcOx & (B) *Cde*AlcOx.** Specific activities were measured by the ABTS/HRP coupled assay using 3 mM BnOH. pH ranging from 4 to 7.5 and 7.5 to 9 were respectively maintained with 50 mM citrate phosphate buffer (blue diamond) and 50 mM Tris-HCl buffers (green circle). *Cta*AlcOx and *Cde*AlcOx were used at 1 nM. Error bars show s.d. (independent experiments, n = 3).

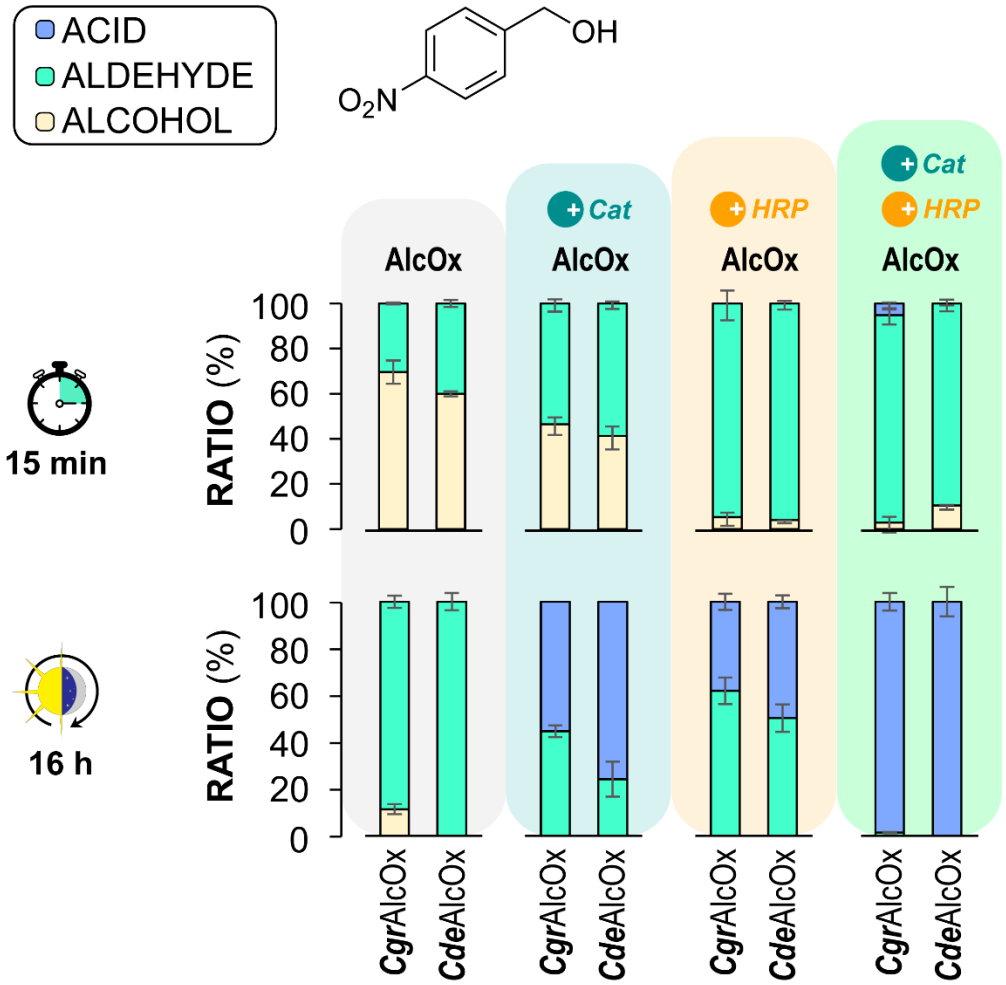


**Figure S8. *Cgr*AlcOx and *Cde*AlcOx mediated oxidation of 4-$NO_2$-BnOH.** Reactions were incubated for either 15 minutes or 16 hours. All reaction mixtures contained: 3 mM substrate and 1 µM AlcOx, in phosphate sodium buffer (50 mM, pH 8.0) and 23°C. Reactions varied as follows: no auxiliary enzyme added, addition of catalase (8 µM final), addition of HRP (12 µM final), addition of both catalase (0.5 µM) and HRP (12 µM final). Conversion products were analyzed by GC-FID. Error bars show s.d. (independent experiments, n = 3).

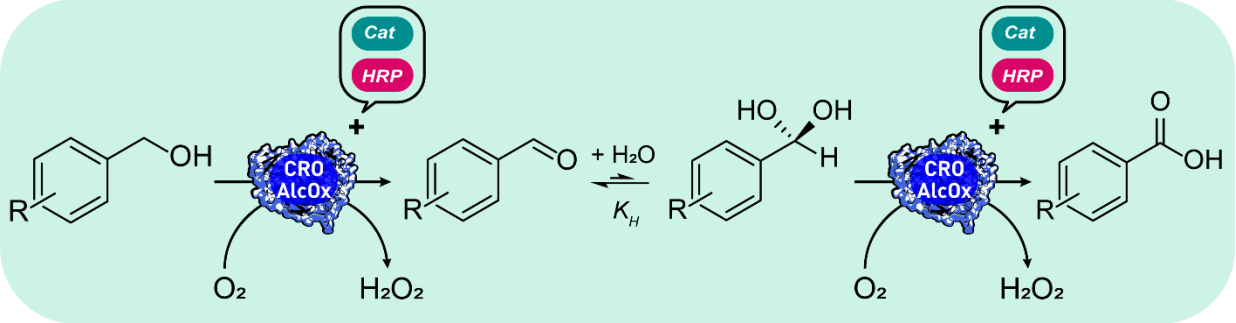


**Scheme S1. Proposed mechanism (based on a previous study** (4)**) for the oxidation of benzyl alcohol derivatives by the *Cgr*AlcOx.**

**Table S1. Top-five of most abundant proteins in *Colletotrichum* secretomes** (according to PAI). Each cell contains the protein type and its JGI accession number (in italic) [a,b]

*C. tabacum*

| | YG | | | YG-CME | | |
|---|---|---|---|---|---|---|
| Rank | d3 | d7 | d14 | d3 | d7 | d14 |
| 1 | L-gulonolactone oxidase; *12384* | CBM1-PL3_2; *10469* | GH72; *10141* | AA9; *4708* | GH17; *3085* | AA9; *4708* |
| 2 | Putative FAD oxidoreductase; *12106* | GH17; *3085* | CBM1-PL3_2; *10469* | AA9; *10008* | AA1_3; *10075* | GH17; *3085* |
| 3 | Feruloyl esterase; *4066* | CE1; *13740* | CE1; *13740* | AA9; *1520* | GH15-CBM20; *11319* | AA5_1; *827* |
| 4 | GH31; *10601* | CE4; *3221* | CBM35-GH26; *14407* | AA1_3; *10075* | PL1_7; *9696* | AA9; *10008* |
| 5 | GH17; *5071* | CBM35-GH26; *14407* | Feruloyl esterase; *4066* | UNK; *11499* | AA9; *10008* | GH15-CBM20; *11319* |

*C. destructivum*

| | YG | | | YG-CME | | |
|---|---|---|---|---|---|---|
| Rank | d3 | d7 | d14 | d3 | d7 | d14 |
| 1 | L-gulonolactone oxidase; *12384* | Adenosylhomocysteinase; *48* | L-gulonolactone oxidase; *12384* | CE4-CBM18-CBM18; *8548* | AA5_1; *827* | UNK; *1971* |
| 2 | Adenosylhomocysteinase; *48* | L-gulonolactone oxidase; *12384* | Putative FAD oxidoreductase; *12106* | L-gulonolactone oxidase; *12384* | L-gulonolactone oxidase; *12384* | AA5_1; *827* |
| 3 | CE5-CBM24-CBM24; *13441* | CE5-CBM24-CBM24; *13441* | GH3; *4665* | UNK; *1987* | CE4-CBM18-CBM18; *8548* | L-gulonolactone oxidase; *12384* |
| 4 | Putative FAD oxidoreductase; *12106* | Putative FAD oxidoreductase; *12106* | Putative peptidase; *590* | GH105; *4860* | AA3_2; *3248* | AA3_2; *3248* |
| 5 | GH17; *3085* | GH17; *5071* | GH15-CBM20; *8930* | Putative serine-protease; *7903* | Putative FAD oxidoreductase; *12106* | Putative FAD oxidoreductase; *12106* |

*C. graminicola*

| | YG | | YG-CME | |
|---|---|---|---|---|
| | d7 | d14 | d7 | d14 |
| 1 | GH28; *4565* | GH28; *4565* | GH28; *4565* | GH28; *4565* |
| 2 | Putative DNase; *11676* | Aminocarboxymuconate-semialdehyde decarboxylase; *8166* | Putative cerato-platanin; *4510* | Putative cerato-platanin; *4510* |
| 3 | GH18; *10483* | Putative DNase; *11676* | UNK; *2752* | GH18; *10483* |
| 4 | Putative sulfhydryl oxidase; *4345* | Putative tannase and feruloyl esterase; *6369* | GH18; *10483* | UNK; *2752* |
| 5 | GH17; *9930* | Putative sulfhydryl oxidase; *4345* | Putative DNase; *11676* | Putative DNase; *11676* |

[a] *"putative" qualifies proteins not annotated in the main analysis and subsequently manually blasted against NCBI database*
[b] *AA enzymes are displayed in red*

**Table S2. GC-programs applied for analysis of the different compounds.**

| Compounds | Rate (°C.min$^{-1}$) | T (°C) | Time (min) |
|---|---|---|---|
| (4-$NO_2$-benzyl-)[1] | - | 130 | 3 |
| | 3 | 180 | 0 |
| | 40 | 220 | 5 |
| (Hexan-)[1] | - | 40 | 4 |
| | 8 | 100 | 0 |
| | 25 | 220 | 3 |
| (Octan-)[1] | - | 80 | 5.5 |
| | 12 | 220 | 3.5 |

[1] Substrate scaffold bearing the primary alcohol, the aldehyde or the carboxylic acid function.

## REFERENCES


1. Mathieu Y, Offen WA, Forget SM, Ciano L, Viborg AH, Blagova E, Henrissat B, Walton PH, Davies GJ, Brumer H. 2020. Discovery of a fungal copper radical oxidase with high catalytic efficiency towards 5-hydroxymethylfurfural and benzyl alcohols for bioprocessing. ACS Catal. 10:3042–3058.

2. Yin D, Urresti S, Lafond M, Johnston EM, Derikvand F, Ciano L, Berrin J-G, Henrissat B, Walton PH, Davies GJ, Brumer H. 2015. Structure–function characterization reveals new catalytic diversity in the galactose oxidase and glyoxal oxidase family. 1. Nat Commun. 6:10197.

3. Kelley LA, Mezulis S, Yates CM, Wass MN, Sternberg MJE. 2015. The Phyre2 web portal for protein modeling, prediction and analysis. 6. Nat Protoc. 10:845–858.

4. Ribeaucourt D, Bissaro B, Guallar V, Yemloul M, Haon M, Grisel S, Alphand V, Brumer H, Lambert F, Berrin J-G, Lafond M. 2021. Comprehensive Insights into the Production of Long Chain Aliphatic Aldehydes Using a Copper-Radical Alcohol Oxidase as Biocatalyst. ACS Sustainable Chem Eng. 9:4411–4421.